

# Structural, magnetic, dielectric and magneto-dielectric coupling analysis of ferromagnetic-PbZr<sub>0.52</sub>Ti<sub>0.48</sub>O<sub>3</sub> nanocomposites

Manish Kumar<sup>1,2,3</sup> · S. Shankar<sup>2,3</sup> · Shiv Kumar<sup>1</sup> · O. P. Thakur<sup>3</sup> · Anup K. Ghosh<sup>1</sup>

Received: 26 January 2016 / Accepted: 4 March 2016 / Published online: 25 March 2016  
© Springer Science+Business Media New York 2016

**Abstract** Nanocomposites of La<sub>0.7</sub>Sr<sub>0.3</sub>MnO<sub>3</sub>-PbZr<sub>0.52</sub>Ti<sub>0.48</sub>O<sub>3</sub> (LSMO-PZT) were synthesized by sol-gel route. The powder X-ray diffraction study confirmed the phase purity and the particle size ( $\approx 30$ – $34$  nm) of the nanocomposites. Magnetic, dielectric and magneto-dielectric studies of LSMO-PZT nanocomposites reflected a coupling between dielectric and magnetic parameters near the magnetic transition temperature ( $T_c \approx 360$  K). The quantitative magneto-dielectric coupling was found to be maximum value of 1.34 in magnitude at 1.5 T and decrease with increase in frequency. This provides the signature of magneto-dielectric coupling qualitatively as well as quantitatively in LSMO-PZT nanocomposites.

## 1 Introduction

Composites of ferromagnetic and ferroelectric compounds have attracted considerable interest because of their tremendous and potential applications [1, 2]. The coupling between electric and magnetic orderings in these materials is remarkably attractive. Magneto-dielectric materials

exhibit the simultaneous presence of magnetic and dielectric orderings in the same crystallographic phase, where magnetic polarization can be induced by the application of electric field and vice versa. These materials have been studied extensively for their various interesting properties in different fields of basic and applied research. This type of materials are the promising materials for their use in data storage, spin valves, quantum electromagnets, microelectronic devices, etc. and are also useful for applications as sensors, waveguides, switches, and modulators [3–6].

Mixed valence perovskite oxides ( $R_{1-x}A_xMO_3$ , where R, A, and M are trivalent rare earth cation, divalent alkaline-earth cations, and transition metal cations, respectively) have attracted great interest due to their rich varieties of interesting properties like magnetic, transport and magneto-dielectric properties, which have immense importance for device applications. Half-metallic ferromagnetic materials La<sub>1-x</sub>Sr<sub>x</sub>MnO<sub>3</sub> exhibit strong ferromagnetism, metallic conductivity, tuned transition temperature ( $T_c$ ) and many other properties. Phase diagram shows the magnetic and metal-insulator transitions [7, 8] that describes the electrical and magnetic properties of La<sub>0.7</sub>Sr<sub>0.3</sub>MnO<sub>3</sub> (LSMO) on the basis of spin configuration and electrical conduction [9–11]. The properties of pure LaMnO<sub>3</sub> change strongly with Sr doping, which introduces holes in the manganese  $e_g$  band ( $Mn^{3+}/Mn^{4+}$  mixed valence state), eventually producing mobile charge carriers i.e. conduction and canting of Mn spins [12–17]. It is particularly attractive due to its highest Curie temperature ( $T_c$ ) in the concentration range where colossal magnetoresistance takes place.

PbZr<sub>0.52</sub>Ti<sub>0.48</sub>O<sub>3</sub> (PZT) is an insulating oxide with perovskite structure which exhibit a unusual morphotropic phase boundary (MPB) between the rhombohedral Zr-rich phase and tetragonal Ti-rich phase, display the maximum

✉ S. Shankar  
sssubramaniam@arsd.du.ac.in

O. P. Thakur  
opthakur@yahoo.com

Anup K. Ghosh  
akghosh@bhu.ac.in

<sup>1</sup> Materials Research Lab, Department of Physics, Banaras Hindu University, Varanasi 221005, India

<sup>2</sup> Department of Physics, ARSD College, University of Delhi, New Delhi 110021, India

<sup>3</sup> Department of Physics, NSIT, New Delhi 110078, India

dielectric, piezoelectric and electromechanical constants along with a high ferroelectric Curie transition temperature of 350 °C [18]. There are some reports on enhanced magneto-dielectric coupling in  $\text{La}_{0.7}\text{Sr}_{0.3}\text{MnO}_3\text{-PbZr}_{0.52}\text{Ti}_{0.48}\text{O}_3$  (LSMO–PZT) multiferroic nanocomposite [19]. The factors which contribute in enhancement of magneto-dielectric coupling (MDC) in LSMO–PZT are connectivity and orientations of the ferroelectric and ferromagnetic phases [20, 21]. Hence, MDC effect in LSMO–PZT nanocomposites is an interesting issue to be solved for device applications. In the present work, we have taken ferromagnetic LSMO nanoparticles and low percentage of ferroelectric PZT nanoparticles to prepare multiferroic nanocomposites and studied the structural, magnetic, magneto-dielectric and transport properties of nanocomposites.

## 2 Experimental

$\text{La}_{0.7}\text{Sr}_{0.3}\text{MnO}_3$  (LSMO) nanoparticles were synthesized using sol–gel technique.  $\text{La}(\text{NO}_3)_3 \cdot 6\text{H}_2\text{O}$ ,  $\text{Sr}(\text{NO}_3)_2$ , and  $\text{Mn}(\text{NO}_3)_2 \cdot 6\text{H}_2\text{O}$  were taken in stoichiometric amounts and dissolved in distilled water under continuous stirring. Citric acid (CA) and ethylene glycol (EG) were added as complexation and polymerization agents, respectively. EG, CA and metal ions were taken in 7:3:1 mol ratio respectively. The clear solution obtained was heated on a hot plate at 80 °C to boil off excess solvent and turned into yellowish gel. The gel was further heated and dried at 200 °C to remove the organic parts. The gel turned into foam, which was decomposed at 400 °C in furnace. The obtained precursor was ground into powder by an agate mortar and was calcined at 600 °C in air atmosphere for 10 h. Calcined powder was then further heat treated at 800 °C for 12 h.

$\text{PbZr}_{0.52}\text{Ti}_{0.48}\text{O}_3$  (PZT) nanoparticles (NP) were prepared from sol–gel route using lead acetate trihydrate [ $\text{Pb}(\text{CH}_3\text{COO})_2 \cdot 3\text{H}_2\text{O}$ ], titanium isopropoxide [ $\text{Ti}(\text{OCH}(\text{CH}_3)_2)_4$ ], Zirconium *n*-propoxide [ $\text{Zr}(\text{OCH}_2\text{CH}_2\text{CH}_3)_4$ ], 70 % 1-propanol, and 2-methoxyethanol ( $\text{CH}_3\text{OC}_2\text{H}_4\text{OH}$ ) as the starting materials to prepare the precursor solutions for PZT–NP drawing. The atomic ratio of the Pb:Zr:Ti of the solution was 1:0.52:0.48. 10 % excess lead acetate was introduced. Stoichiometric amounts of Lead acetate and Zirconium *n*-propoxide were dissolved in 2-methoxyethanol under stirring at room temperature separately. Required amount of titanium isopropoxide were then added to the Zirconium solution with addition of some small amount of solvent under stirring to prepare Zr–Ti solution. While stirring the Zr–Ti solution, Pb solution was added into it and heated at 60 °C for 30 min. The pH of the solution had been adjusted to 5 by adding some water. After few minutes the color of the solution becomes milky

white and becomes gelatinous. The gel was heated at 60 °C for 48 h and then calcined at 700 °C for 1 h to get PZT powders.

PZT nanoparticles with amount 1, 2 and 5 % were mixed with 99, 98 and 95 % LSMO nanoparticles respectively. Samples have been named according to the percentage of PZT present in composite as LP0 (pure LSMO), LP1 (1 % PZT), LP2 (2 % PZT) and LP5 (5 % PZT). All the mixed systems were then pelletized and heat treated at 700 °C for 2 h. X-ray diffraction had been done by Rigaku Miniflex II DEXTOP X-ray diffractometer with Cu-K $\alpha$  radiation. Temperature dependent magnetic measurements were done using Vibrating Sample Magnetometer (Lake-shore: Model no. 7407). Dielectric measurements were made over the temperature range 300–400 K at fixed frequencies of 10 kHz, 100 kHz and 1 MHz using Agilent Precession LCR Meter E4980A and over the frequency range 10 Hz–1 MHz at 360 K using Nova Control (Alpha-A) high performance frequency analyzer.

## 3 Results and discussion

The phase purity of LSMO–PZT nanocomposites (LP0, LP1, LP2, LP5 and PZT) is studied by powder X-ray diffraction (XRD) patterns as shown in the Fig. 1. For the composite samples, the XRD patterns can be indexed to two set of diffraction peaks corresponding to LSMO and PZT phases. Miller indices (hkl) of the diffraction peaks of LSMO and PZT are matched with JCPDS card numbers 00-051-0409 and 33-0784 respectively. Powder XRD patterns confirm that there is no appearance of any impurity peaks in pure rhombohedral structure LSMO (space group  $R\bar{3}c$ ) and PZT (space group, P4 mm). The XRD patterns clearly show the presence of PZT peak ( $2\theta = 31.25^\circ$ ) in all the nanocomposites (LP1, LP2 and LP5) and is indicated

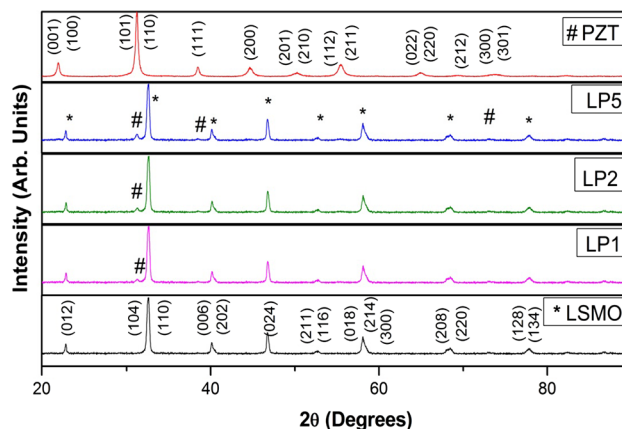


**Fig. 1** Powder XRD patterns of LSMO–PZT (LSMO, PZT, LP1, LP2 and LP5) nanocomposites

by ‘#’ in Fig. 1. The average particle size of LP0, LP1, LP2, LP5 and PZT nanocomposites, estimated using the Debye–Scherer’s formula [22], were ranging between 30–34 nm respectively. The diffraction peaks of LSMO in all composites did not shift, indicating that after sintering the cell parameters of the LSMO remains unchanged due to the small amount of PZT content and that the reactions between LSMO and PZT grains are small but countable. With the increase of PZT content, the intensity of the LSMO peaks are unchanged, so that it can be suggested that the composites are not homogeneous granular systems and it also confirms the countable reaction between LSMO and PZT grains.

Figure 2 shows the plot of inverse of susceptibility with the variation of temperature ( $\frac{1}{\chi}$  vs  $T$ ) for LP5 at a field of 5000 Oe in the temperature range of 300–400 K. The extrapolation of the straight line fit to the high temperature region gives a magnetic transition temperature,  $T_c \approx 360$  K. The transition temperature is also same nearly 360 K for pure LP0 and other nanocomposites (LP1 and LP2) as shown in the Table 1. It should be pointed out that the transition temperature does not vary appreciably with the variation of low amount of PZT concentration, which implies that addition of PZT does not affect the intrinsic property of LSMO.

The dielectric parameters i.e. dielectric constant ( $\epsilon'$ ) and dielectric loss ( $\tan \delta$ ) are measured at the magnetic transition temperature  $T_c \approx 360$  K in the frequency (10 Hz–1 MHz) range respectively. The dependence of the dielectric constant ( $\epsilon'$ ) and dielectric loss ( $\tan \delta$ ) on the applied field frequency ( $f$ ) for LSMO–PZT composites is shown in Fig. 3a, b. All nanocomposites show dispersion in dielectric constant and dielectric loss at low frequency and

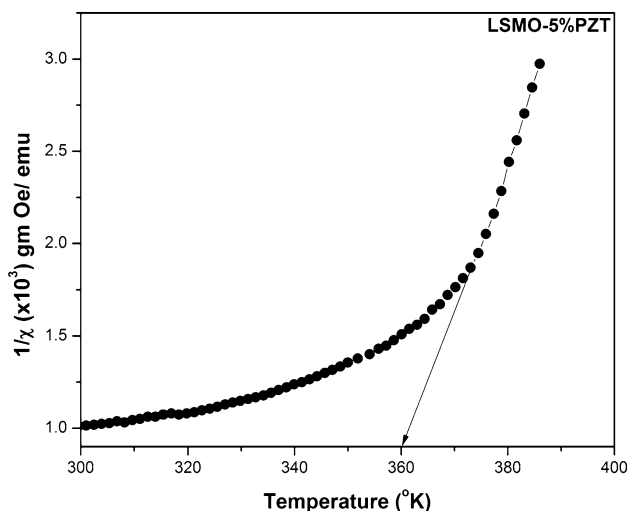


Fig. 2 Variation of  $\frac{1}{\chi}$  vs  $T$  for LP5 nanocomposite

Table 1 %MDE of LP5 composition at different fixed frequencies (1 kHz, 10 kHz and 1 MHz) at 1.5 T

LP5 composition at 1.5 T	
Frequency	% MDE (magnitude)
1 kHz	1.34
10 kHz	1.14
1 MHz	0.69

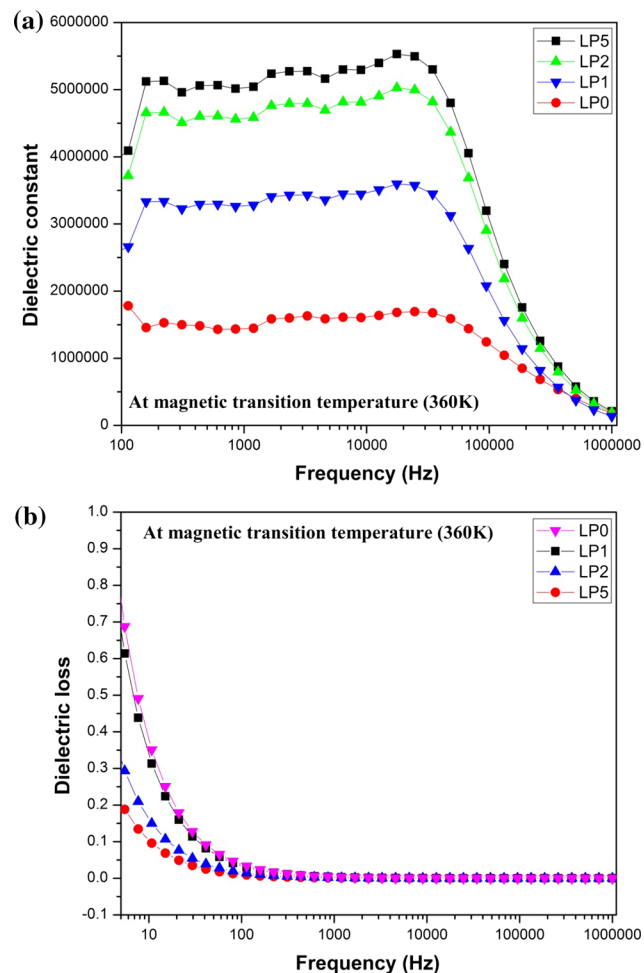
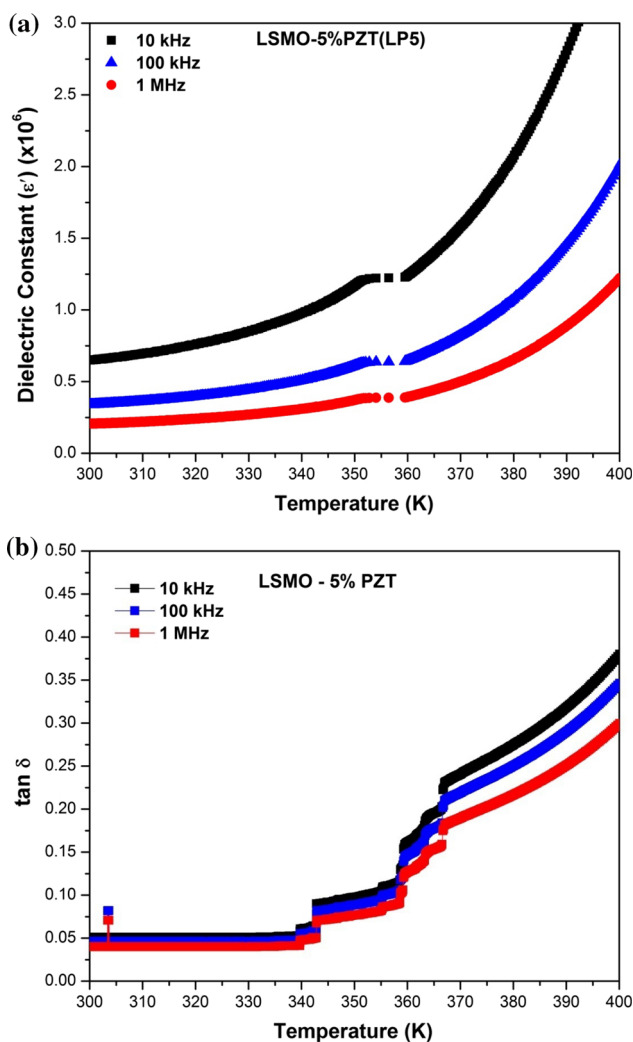


Fig. 3 a Variation of dielectric constant with respect to frequency of LP0, LP1, LP2 and LP5 nanocomposites. b Variation of dielectric loss with respect to frequency of LP0, LP1, LP2 and LP5 nanocomposites

the dielectric constant shows very high values, which is attributed to the interfacial/space charge polarization [23, 24]. Dielectric constant remains almost constant over the range 200 Hz–5 kHz indicating the use of these LSMO–PZT nanocomposites in bandpass filters. The dielectric constant of LSMO–PZT system increase with increase in content of PZT, as shown in Fig. 3a and the achieved

values are comparable to earlier reported values [25, 26]. The dielectric loss ( $\tan \delta$ ) values decrease as frequency increases up to 500 Hz and become more or less constant up to 1 MHz for all nanocomposites, as shown in Fig. 3b. This observation may be explained by the phenomenon of dipole relaxation. This is due to the incapability of the electric dipoles to be in pace with the frequency of applied electric field [27].

The dielectric constant and the loss tangent are measured for LP5 nanocomposite as a function of temperature from 300 to 400 K at 10 kHz, 100 kHz and 1 MHz as shown in Fig. 4a, b. The dielectric constant increases with increasing temperature in a characteristic manner indicating a presence of interfacial/space charge polarization, as shown in Fig. 4a. The dielectric constant plot for the composite exhibit a clear anomaly near the magnetic transition temperature ( $T_c \approx 360$  K) and it is independent



**Fig. 4** a Variation of dielectric constant with respect to temperature of LP5. b Variation of dielectric loss with respect to temperature of LP5

of frequency. However, it could be seen that dielectric constant reduces with increasing frequency. The anomaly is also strongly reflected in the dielectric loss plot at  $T_c \approx 360$  K and is also independent of frequency as shown in inset of Fig. 4b. The dielectric anomaly at magnetic transition temperature can be attributed to the magneto-dielectric coupling (MDC) qualitatively and has also been reported in some of the single phase and composite multiferroics [28, 29]. This coupling can be assumed to arise from two contributions mainly parent LSMO nano grains and other due to PZT at LSMO grain boundaries occurring as a result of differences in conductivities of LSMO and PZT nanoparticles. In other compositions (LP0, LP1 and LP2) a parallel behaviour is observed with decreasing value of dielectric constant for decreasing concentration.

The MDC is quantified by measuring the dielectric constant of LP5 nanocomposite at magnetic transition temperature ( $T_c \approx 360$  K) as a function of the magnetic field at 10 kHz, 100 kHz and 1 MHz. The MDC effect is calculated using the following relation:

$$\%MDC = [\epsilon'(H) - \epsilon'(0)]/\epsilon'(H) \times 100 \quad (1)$$

where  $\epsilon'(H)$  and  $\epsilon'(0)$  are the dielectric constants with and without magnetic fields, respectively. Figure 5 shows the plot of %MDC as a function of magnetic field at 10 kHz, 100 kHz and 1 MHz. The %MDC is found to be maximum value of 1.34 in magnitude at 1.5 T ( $\approx 15$  kOe) and decrease with increase in frequency as shown in the Table 1. This is the maximum possible MDC value at 10 kHz because near the transition temperature LSMO–PZT composites exhibits high magnetostriction which enhances the strain mediated coupling [30]. The values of obtained %MDC for LSMO–PZT composites is

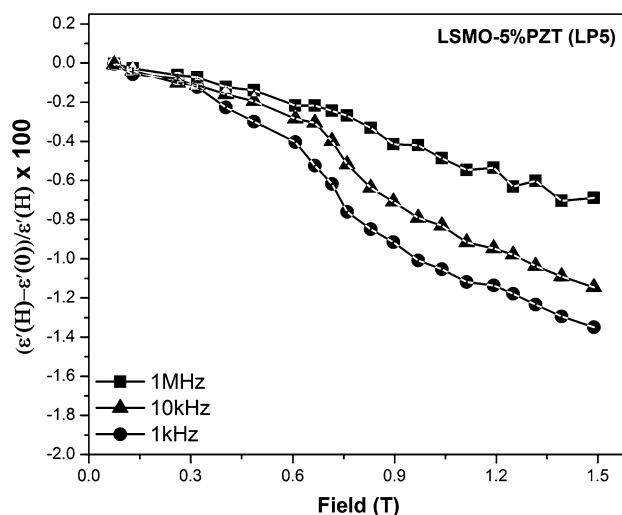


**Fig. 5** Variation of percentage change in dielectric constant as a function of magnetic field i.e. %MDC at frequencies of 1 MHz, 10 kHz and 1 kHz

significantly large than those reported for LSMO based composites [11, 31, 32] where the MDC is observed for relatively lower field. The other compositions (LP1 and LP2) exhibit a parallel behaviour with decreasing value of %MDC for decreasing concentration.

#### 4 Conclusion

In summary, LSMO–PZT nano particles were successfully synthesized by sol–gel route. The results obtained from the powder XRD confirmed the formation of the desired crystallographic phases ( $R\bar{3}c$  and P4 mm space group) of LSMO, PZT and LSMO–PZT nanocomposites with average particle size ranging between 30 and 34 nm. The clear anomaly of dielectric constant near the magnetic transition temperature ( $T_c \approx 360$  K) and the % MDC measurement confirmed the magneto-dielectric coupling in LSMO–PZT nanocomposites. To conclude our results provide the enhanced structural, magnetic and dielectric properties with the signature of qualitative as well as quantitative magneto-dielectric coupling in the LSMO–PZT nanocomposites.

**Acknowledgments** The authors would like to thank Department of Ceramic Engineering, IIT(BHU), Varanasi, India for their characterization facilities.

#### References

- D. Kathrin, J. Phys. D Appl. Phys. **39**, R125 (2006)
- O.M. Hemeda, A. Tawfik, A. Al-Sharif, M.A. Amer, B.M. Kamal, D.E. El Refaay, M. Bououdina, J. Magn. Magn. Mater. **324**, 4118 (2012)
- W. Eerenstein, N.D. Mathur, J.F. Scott, Nature **442**, 759 (2006)
- F. Zavaliche, T. Zhao, H. Zheng, F. Straub, M.P. Cruz, P.L. Yang, D. Hao, R. Ramesh, Nano Lett. **7**, 1586 (2007)
- N.A. Spaldin, M. Fiebig, Science **309**, 391 (2005)
- I. Kornev, M. Bichurin, J.P. Rivera, S. Gentil, H. Schmid, A.G.M. Jansen, P. Wyder, Phys. Rev. B **62**, 12247 (2000)
- A. Urushibara, Y. Moritomo, T. Arima, A. Asamitsu, G. Kidon, Y. Tokura, Phys. Rev. B **51**, 14103 (1995)
- J.S. Zhou, J.B. Goodenough, Phys. Rev. B **64**, 024421 (2001)
- P.T. Phong, D.H. Manh, P.H. Nam, D.K. Tung, N.X. Phuc, I.J. Lee, Phys. B **444**, 94 (2014)
- C. Thirnal, C. Nayek, P. Murugavel, V. Subramanian, AIP Adv. **3**, 112109 (2013)
- M. Kumar, S. Shankar, G.D. Dwivedi, A. Anshul, O.P. Thakur, A.K. Ghosh, Appl. Phys. Lett. **106**, 072903 (2015)
- C. Zener, Phys. Rev. **82**, 403 (1951)
- P.W. Anderson, H. Hasegawa, Phys. Rev. **100**, 675 (1955)
- P.G. de Gennes, Phys. Rev. **100**, 564 (1955)
- N. Furukawa, J. Phys. Soc. Jpn. **64**, 3164 (1995)
- M. Jaime, P. Lin, M.B. Salamon, P.D. Han, Phys. Rev. B **58**, R5901 (1998)
- A.P. Ramirez, J. Phys.: Condens. Matter **9**, 8171 (1997)
- Y.S. Hoon, S.H. Kim, S.J. Lee, H.K. Kim, M. Lee, J. Sens. Actuators A **125**, 463 (2006)
- Z.H. Tang, M.H. Tang, X.S. Lv, H.Q. Cai, Y.G. Xiao, C.P. Cheng, Y.C. Zhou, J.J. He, Appl. Phys. **113**, 164106 (2013)
- J. Ma, J.M. Hu, Z. Li, C.W. Nan, Adv. Mater. **23**(9), 1062 (2011)
- G.D. Dwivedi, M. Kumar, P. Shahi, A. Barman, S. Chatterjee, A.K. Ghosh, RSC Adv. **5**, 30748 (2015)
- B.D. Cullity, Elements of X-Ray Diffraction, Addison-Wesley:MA1978
- H.Y. Hwang, S.W. Cheong, N.P. Ong, B. Batlogg, Phys. Rev. Lett. **77**, 2041 (1996)
- J. Kaur, V. Gupta, R.K. Kotnala, K.C. Verma, Ind. J. Pure Appl. Phys. **50**, 57 (2012)
- Z. Zalita, S.A. Halim, W.D.W. Yusoff, Z.A. Talib, K.P. Lim, M. Mazni, Solid State Sci Technol **19**(1), 169 (2011)
- M.P. Gutiérrez, J. Mira, J. Rivas, Phys. Lett. A **323**, 473 (2004)
- S. Shankar, M. Kumar, A.K. Ghosh, O.P. Thakur, J. Mater. Sci.: Mater. Electron **25**, 4896 (2014)
- T. Kimura, S. Kawamoto, I. Yamada, M. Azuma, M. Takano, Y. Tokura, Phys. Rev. B **67**, 180401(R) (2003)
- M.A. Zurbuchen, T. Wu, S. Saha, J. Mitchell, S.K. Streiffer, Appl. Phys. Lett. **87**, 232908 (2005)
- T. Kimura, S. Kawamoto, I. Yamada, M. Azuma, M. Takano, Y. Tokura, Phys. Rev. B **67**, 180401 (2003)
- M.M. Sutar, A.N. Tarale, S.R. Jigajeni, S.B. Kulkarni, P.B. Joshi, Appl. Nanosci. **2**, 311 (2012)
- N. Tarale, P.B. Joshi, S.B. Kulkarni, V.R. Reddy, M. Gupta, R.C. Pawar, C.S. Lee, J. Sol-Gel Sci. Tech. **70**, 346 (2014)